metal with respect to the ring system is consistent with theoretical studies.

Although these NMR studies offered no direct evidence for intermediate species of reduced hapticity in the arene systems, the observation of intermediates in the reactions of the azulene complexes in CH_2Cl_2 solutions with the very weak nucleophile CO and the rapidity of the reactions indicate that the mechanism for arene replacement in this case quite likely occurs through an $\eta^5 \rightleftharpoons \eta^3$ preequilibrium. The trapping efficiency of the weak nucleophile CO at low concentrations suggests that kinetic measurements conducted on the reaction of the Ru–azulene systems with better nuclephiles at high concentration may show the expected saturation effect and further support the operation of a $\eta^6 \rightleftharpoons \eta^4$ preequilibrium in the arene systems.

Acknowledgment. A.M.M. acknowledges a Louise T. Dosdall Fellowship in Science. This research was supported by Department of Energy Grant DOE/DEAC02-83ER13103. The Cary Model 17-D spectrometer was made available by funding received in part from the National Science Foundation (Grant CHE-23857).

Registry No. $[(\eta^5\text{-}C_5H_5)Ru(\eta^6\text{-}C_{10}H_8)]PF_6$, 102538-40-9; $[(\eta^5\text{-}C_5H_5)Ru(\eta^6\text{-}C_{14}H_{10})]PF_6$, 102575-39-3; $[(\eta^5\text{-}C_5H_5)Ru(\eta^6\text{-}C_{16}H_{10})]PF_6$, 102575-41-7; $[(\eta^5\text{-}C_5H_5)Ru(\eta^6\text{-}C_{18}H_{12})]PF_6$, 102538-42-1; $[(\eta^5\text{-}C_5H_5)Ru(\eta^5\text{-}C_{10}H_8)]PF_6$, 102538-44-3; $[(\eta^5\text{-}C_5(CH_3)_5)Ru(\eta^6\text{-}C_{10}H_8)]PF_6$, 102575-43-9; $[(\eta^5\text{-}C_5(CH_3)_5)Ru(\eta^6\text{-}C_{14}H_{10})]PF_6$, 102575-45-1; $[(\eta^5\text{-}C_5(CH_3)_5)Ru(\eta^6\text{-}C_{16}H_{10})]PF_6$, 102575-47-3; $[(\eta^5\text{-}C_5(CH_3)_5)Ru(\eta^6\text{-}C_{18}H_{12})]PF_6$, 102538-46-5; $[(\eta^5\text{-}C_5(CH_3)_5)Ru(\eta^5\text{-}C_{10}H_8)]PF_6$, 102575-49-5; $[(\eta^5\text{-}C_5H_5)Fe(\eta^6\text{-}C_{18}H_{12})]^+$, 92140-26-6; $[(\eta^5\text{-}C_5H_5)Fe(\eta^6\text{-}C_{16}H_{10})]^+$, 70755-98-5; $[(\eta^5\text{-}C_5H_5)Ru(CH_3CN)_3]PF_6$, 80049-61-2; $[(\eta^5\text{-}C_5(CH_3)_5)Ru(CH_3CN)_3]PF_6$, 99604-67-8; $[(\eta^5\text{-}C_5(CH_3)_5)Ru(\eta^6\text{-}C_6H_6)]PF_6$, 99631-48-8; $[(\eta^5\text{-}C_5H_5)Ru(CO)_3]PF_6$, 31741-71-6; $[(\eta^5\text{-}C_5(CH_3)_5)Ru(CO)_3]PF_6$, 102538-47-6; $[(\eta^5\text{-}C_5H_5)Ru(CD_3CN)_3]PF_6$, 102538-49-8; $[(\eta^5\text{-}C_5(CH_3)_5)Ru(CD_3CN)_3]PF_6$, 102538-51-2.

Supplementary Material Available: ^1H NMR spectra of $[(\eta^5\text{-}C_5(CH_3)_5)Ru(\eta^6\text{-anthracene})]^+$, $[(\eta^5\text{-}C_5H_5)Ru(\eta^6\text{-pyrene})]^+$, and $[(\eta^5\text{-}C_5H_5)Ru(\eta^6\text{-chrysene})]^+$ (3 pages). Ordering information is given on any current masthead page.

Contribution from the Department of Chemistry, University of Houston, Houston, Texas 77004

Polyaza Cavity-Shaped Molecules. 9. Ruthenium(II) Complexes of Annelated Derivatives of 2,2′:6,2″-Terpyridine and Related Systems: Synthesis, Properties, and Structure

Randolph P. Thummel* and Yurngdong Jahng

Received November 15, 1985

Annelated derivatives of 2,2′:6,2″-terpyridine and their dibenzo- and dipyrido-fused analogues coordinate with ruthenium(II) in an octahedral fashion even when the conformation of the free ligand is highly distorted from planarity. NMR chemical shift data have been used as a sensitive probe of shielding and deshielding effects dependent upon the relative orientation of the terpyridine ligands about the metal atom. An X-ray structure has been determined for the complex $Ru(\mathbf{1d})_2[PF_6]_2$ with the molecular formula $C_{48}H_{52}F_{12}N_6OP_2Ru$, which crystallizes in the triclinic space group $P\bar{1}$ with two molecules per unit cell and a = 10.237 (1) Å, b = 13.250 (1) Å, c = 19.761 (3) Å, α = 73.59 (1)°, β = 89.59 (1)°, and γ = 72.22 (1)°. Coordination of ruthenium(II) with the bis(tetramethylene)-bridged terpyridine **1d** does not greatly alter the geometry of complexation at the metal center. Instead the ligand distorts to accommodate coordination and a substantial degree of this distortion is manifested by nonplanarity in the individual pyridine rings. Despite these changes, which might be expected to affect the electronic properties of the complex, no dramatic differences are observed in the electronic absorptions as a function of bridge length.

Introduction

When pyridine rings are bonded to one another through their 2- and/or 6-positions, a situation is created where trigonal nitrogen atoms are joined in a 1,4-fashion that is particularly favorable to metal chelate ring formation. The prototypical example is 2,2′-bipyridine, which is known to form a wide variety of bidentate metal complexes. The next higher homologue, 2,2′:6,2″-terpyridine,[1] is also an excellent ligand, which can act in a tridentate fashion, forming two five-membered chelate rings that share a common bond between the metal and central nitrogen.

Two important observations can be made regarding terpyridine as a ligand. In its uncomplexed form this molecule is postulated to exist in an anti-anti conformation in which the H–H and

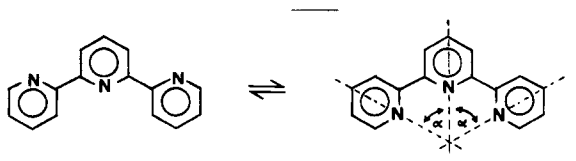

anti-anti syn-syn

nitrogen lone-pair repulsions are minimized.[2] To coordinate effectively terpyridine must adopt the syn-syn conformation. Relatively free rotation about the 2,2′- and 6,2″-bonds make this conformation readily accessible. If one assumes an unperturbed hexagonal geometry for the pyridine rings, the locus of the axes passing through the center of each ring would be significantly outside the cavity of the molecule. If a metal atom were to be located at this locus, coplanar with and equidistant from all three pyridines, the N–M–N bond angles (α) would be about 60°, which is substantially distorted from the orthogonality preferred by octahedral metal complexes.

We have recently synthesized a series of bisannelated terpyridines (**1b–d**) in which the relative orientation of the three connected pyridine rings is controlled by polymethylene bridges between the 3,3′- and 5,3″-positions. Both the dihedral angles

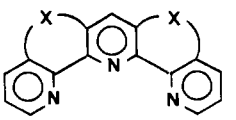

1a, X = H, H
b, X = $(CH_2)_2$
c, X = $(CH_2)_3$
d, X = $(CH_2)_4$

(1) The central ring of terpyridine is assigned unprimed numbers to preserve consistency among structures **1**, **2**, and **3**.

(2) Nakamoto, K. *J. Phys. Chem.* **1960**, *64*, 1420.

0020-1669/86/1325-2527$01.50/0

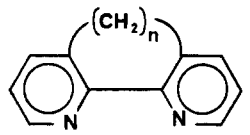

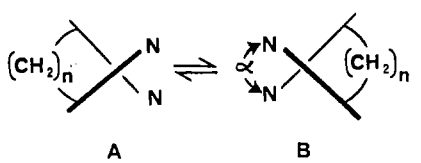

n	α
1	0°
2	20
3	55
4	80

A B

Figure 1. Dependence of dihedral angle on bridge length for 3,3′-annelated azabiaryls.

between adjacent pyridine rings and the "bite angle" α of a five-membered chelate ring will be determined by the length of these methylene bridges. In an earlier paper we have presented the synthesis and conformational properties of the terpyridines **1b–d** as well as bridged derivatives of their related dibenzo- and dipyrido-fused analogues **2** and **3**.[3] In this work we will describe the biscoordination of these ligands with ruthenium(II).

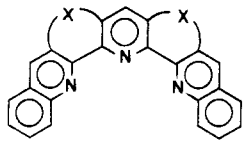

2a, X = H, H
b, X = $(CH_2)_2$
c, X = $(CH_2)_3$
d, X = $(CH_2)_4$

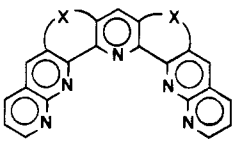

3a, X = H, H
b, X = $(CH_2)_2$
c, X = $(CH_2)_3$
d, X = $(CH_2)_4$

The $Ru(tpy)_2^{2+}$ complex was first prepared in 1932 by Morgan and Burstall,[4] and a good deal of work has been reported concerning the photophysical and electrochemical properties of this system.[5-13] Iron(II),[14] ruthenium(II),[15] and osmium(II)[15] complexes of 2,6-di-2′-quinolylpyridine (**2a**) have been reported, and the possible steric effects of dibenzo substitution on the physical properties of these systems have been pointed out.

Examination of molecular models for a series of 3,3′-polymethylene-bridged 2,2′-bipyridines indicates the relationship of the dihedral angle between the two pyridine rings and the length of the bridge to be as shown in Figure 1. The barrier to interconversion of A and B is sufficiently low at room temperature that the molecules with two- and three-carbon bridges are conformationally mobile on the NMR time scale.[16] For the $n = 4$ system, however, the molecule is conformationally rigid by NMR. In the terpyridine series this has led to the detection of diastereomeric *dl* and meso forms of the doubly bridged system **1d**:[3]

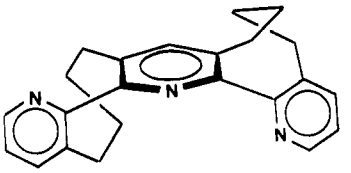

dl form

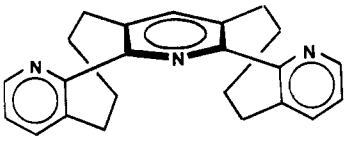

meso form

At low temperatures, similar forms of **1b** and **1c** would presumably be observable.

Once again an examination of molecular models highlights some interesting conformational features of these biannelated systems. Table I outlines estimated key interatomic distances for [3,3′:5,3″] bisannelated 2,6-di-2′-quinolylpyridines. When all three aromatic portions of this molecule are forced to lie in the same plane, the length of the polymethylene bridge exerts a dramatic effect on the N′–N″ and $H_{8'}$–$H_{8''}$ distances as well as the bite angle α. For a monomethylene bridge ($n = 1$), which can only be planar, the two appended quinoline rings are pulled apart from one another and the N′–N″ distance measures 6.0 Å while the bite angle is only 36°. At the other extreme, a trimethylene bridge ($n = 3$) pushes two coplanar quinoline rings toward one another, decreasing the N′–N″ distance to 3.6 Å and opening the bite angle to 81°. The $H_{8'}$–$H_{8''}$ distance is correspondingly large for the former system (8.9 Å) and very short (2.4 Å) for the latter. When the bridges contain four methylene units ($n = 4$) the compression effect is modified somewhat. The additional $-CH_2-$ group in the bridge allows additional degrees of freedom, which diminishes bending of the 2,2′- and 6,2″-bonds. The bite angle accordingly decreases to 77°, somewhat closer to the 57° found in an unstrained system (**1b**). The behavior of the dimethylene-bridged system would be intermediate between that of its two nearest homologues. It is interesting to note that the *dl* form of the tetramethylene-bridged

Table I. Estimated[a] Bite Angles (±2°), Dihedral Angles (±2°), and Key Interatomic Distances (±0.1 Å) for [3,3′:5,3″] Bisannelated 2,6-Di-2′-quinolylpyridines

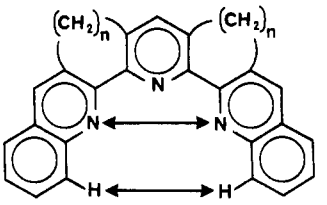

n	conformation	α[b]	θ[c]	N′–N″	$H_{8'}$–$H_{8''}$
1	planar	36	0	6.0	8.9
2	planar	60	0	4.6	4.6
2	meso			4.8	5.6
2	*dl*		39	4.9	6.0
3	planar	81	0	3.6	2.4
3	meso			5.2	6.8
3	*dl*		85	5.7	8.7
4	planar	77	0	3.8	2.7
4	meso			5.8	8.1
4	*dl*		117	6.3	10.4

[a] Measured from Dreiding and Feiser models. [b] Bite angle between axes passing through N and C_4 of adjacent pyridine rings. [c] Dihedral angle between the planes of the two quinoline rings.

(3) Thummel, R. P.; Jahng, Y. *J. Org. Chem.* **1985**, *50*, 2407.
(4) Morgan, G.; Burstall, F. H. *J. Chem. Soc.* **1937**, 1649.
(5) Kirchhoff, J. R.; McMillian, D. R.; Marnot, P. A.; Sauvage, J.-P. *J. Am. Chem. Soc.* **1985**, *107*, 1138.
(6) Morris, D. E.; Hanck, K. W.; DeArmond, M. K. *J. Electroanal. Chem. Interfacial Electrochem.* **1983**, *149*, 115.
(7) Stone, M. L.; Crosby, G. A. *J. Chem. Phys.* **1968**, *48*, 1853.
(8) Creutz, C.; Chou, M.; Netzel, T. L.; Okumura, M.; Sutin, N. *J. Am. Chem. Soc.* **1980**, *102*, 1309.
(9) Young, R. C.; Nagle, J. K.; Meyer, T. J.; Whitten, D. G. *J. Am. Chem. Soc.* **1978**, *100*, 4773.
(10) Ciantelli, G.; Legittimo, P.; Pantani, F. *Anal. Chim. Acta* **1971**, *53*, 303.
(11) Tokel-Takvoryan, N. E.; Hemingway, R. E.; Bard, A. J. *J. Am. Chem. Soc.* **1973**, *95*, 6582.
(12) Kamra, L. C.; Ayres, G. H. *Anal. Chim. Acta* **1976**, *81*, 117.
(13) McHatton, R. C.; Anson, F. C. *Inorg. Chem.* **1984**, *23*, 3935.
(14) Harris, C. M.; Patil, H. R. H.; Sinn, E. *Inorg. Chem.* **1969**, *8*, 101.
(15) Klassen, D. M.; Hudson, C. W.; Shaddix, E. L. *Inorg. Chem.* **1975**, *14*, 2733.
(16) Thummel, R. P.; Lefoulon, F.; Mahadevan, R. *J. Org. Chem.* **1985**, *50*, 3824.

Table II. Selected Proton Chemical Shift Data[a] for RuL_2^{2+} Systems and the Corresponding Ligands (L)[b]

	terpyridine (**1**)		diquinolylpyridine (**2**)		di[1,8]-naphthyridylpyridine (**3**)	
	$H_{6'}$	H_4	$H_{8'}$	H_4	$H_{7'}$	H_4
L (unbridged)	8.70	7.96	8.22	8.07	9.27	8.96–8.02[d]
RuL_2	7.34	8.42	6.52	8.84	8.18	8.66
$\Delta\delta$	−1.36	+0.46	−1.70	+0.77	−1.09	
L (n = 2)	8.72	7.44	8.50	7.32	8.85	7.53
RuL_2	7.17	7.83	6.58	8.40	8.23	8.15
$\Delta\delta$	−1.55	+0.39	−1.92	+1.08	−0.62	+0.62
L (n = 3)	8.71	7.48	8.40	7.53	9.15	7.53
RuL_2	7.13	7.94	6.42	8.30	8.26	8.28
$\Delta\delta$	−1.58	+0.46	−1.98	+0.77	−0.89	+0.75
L (n = 4) meso	8.62	7.50	8.32	7.56	9.18	7.62
dl	8.59	7.52	8.14		9.06	7.58
RuL_2	6.90	7.84	6.42	8.24	8.27	8.16
$\Delta\delta$	−1.70[c]	+0.31[c]	−1.81[c]	+0.68	−0.85[c]	+0.56[c]

[a] Chemical shifts in ppm downfield from Me_4Si. Ligand spectra were obtained in $CDCl_3$ and complexes in CD_3CN. No appreciable solvent shift was observed. [b] Numbering pattern shown in numbered structures. [c] Average difference from meso and *dl* forms. [d] Obscured in multiplet.

species has the largest dihedral angle (117°) between the two quinoline rings yet almost the same N′–N″ distance as the monomethylene derivative, where the quinoline rings are coplanar.

It seems evident that, in order for efficient complexation to occur, the nonplanar terpyridines must become coplanar at the expense of increased strain in the polymethylene bridge. Alternatively, the metal atoms may have to accommodate a coordination geometry that deviates substantially from the preferred octahedral situation. The purpose of this study will be to carefully evaluate the relationships between ligand conformation and coordination geometry.

Synthesis

The ruthenium complexes were prepared by the reaction of 2.5 equiv of ligand with 1.0 equiv of ruthenium trichloride trihydrate in ethanol-water (1:1) followed by precipitation as the hexafluorophosphate salt. Purification was carried out by chromatography or recrystallization. The complexes were characterized primarily by their 300-MHz ^1H NMR spectra, where nearly all proton resonances were readily assignable and peak intensities were in accordance with the proposed structures. Thermospray interfaced LC–MS was employed in many cases to observe the singly charged RuL_2^+ and doubly charged RuL_2^{2+} ions of the complex.

The yields of isolated complexes were generally in excess of 65%. Notable exceptions were the bridged quinolyl systems **2b–d** (15–35%), where the congestion imposed by $H_{8'}$ and $H_{8''}$ with the central ring of the orthogonal ligand may account for the low yields. The yield of $Ru(\mathbf{3d})_2^{2+}$ is also low (20%), possibly due to the considerable nonplanarity of the parent ligand, coupled with increased congestion due to the fused pyrido rings and diminished basicity of the naphthyridine ring system.

Properties

NMR Spectra. Table II summarizes selected proton chemical shift data for the complexes and their corresponding ligands. The chemical shift changes upon complexation for certain protons of the ligand are very diagnostic of their environment. Of primary interest are $H_{6'}$ and H_4 for the terpyridine complexes, $H_{8'}$ and H_4 for the diquinolylpyridine complexes, and $H_{7'}$ and H_4 for the di[1,8]naphthyridylpyridine complexes. Figure 2 illustrates the geometry of an octahedral bis(terpyridine) complex. The proton $H_{6'}$ is held approximately over the plane of the central pyridine ring of the orthogonal ligand. An upfield shift of 1.36–1.70 ppm is observed due to shielding of this proton.

We have hypothesized that for a planar conformation of the ligand the bite angle α will increase and the N′–N″ distance will decrease with increasing length of the polymethylene bridge. A result of this distortion will be to push $H_{6'}$ deeper into the face of the opposing central pyridine ring and hence increase its

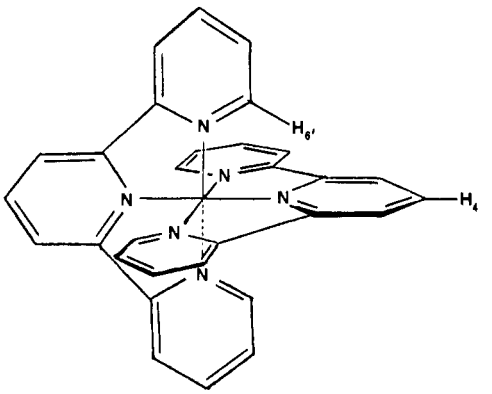

Figure 2. Octahedral coordination geometry of bis(2,2′:6,2″-terpyridine)metal complexes.

shielding. In fact, a regular increase in the upfield shift is observed as one proceeds from the unbridged parent system, $Ru(tpy)_2^{2+}$, to its 3,3′-tetramethylene-bridged analogue.

Similarly, H_4 on the central pyridine ring is held in the deshielding plane of the two terminal pyridine rings of the orthogonal ligand. The chemical shift of this proton therefore moves to lower field upon complexation by about 0.31–0.46 ppm. This deshielding effect becomes more apparent for the diquinolylpyridine systems, where H_4 is considerably closer to the deshielding region of the benzo portion of the opposing quinoline rings and shifts range from 0.68–1.08 ppm. The effect is greatest for n = 2, where coplanarity of the ligand and the "pinching effect" both function to a maximum extent. For the n = 3 and n = 4 systems the steric congestion imposed by the quinoline ring as well as the torsional strain in the bridge probably cause some noncoplanarity of the ligand such that H_4 no longer lies directly in the plane of the quinoline ring. A maximum shift is observed for the n = 3 system.

These same two effects are manifested in the di[1,8]-naphthyridylpyridine complexes but to an intermediate degree. The $H_{7'}$ proton is oriented at the same angle as $H_{6'}$ in the terpyridine series, but as a result of pyrido annelation it is held more directly over the opposing central pyridine ring. The observed shielding effect varies from 0.62 to 1.09 ppm. It is now the unbridged system that shows the largest shift. This observation might be explained by the fact that $H_{8'}$ (and $H_{8''}$) are no longer present in these systems and hence there is less congestion resulting from complexation and the ligand may be most coplanar for the unbridged species, allowing $H_{7'}$ to point more directly toward the shielding region of the opposing pyridine ring.

The conformational properties of the free ligands **1–3** have been carefully analyzed by examining the NMR resonances of their polymethylene bridge protons.[3] The dimethylene- and trimethylene-bridged systems were found to be conformationally

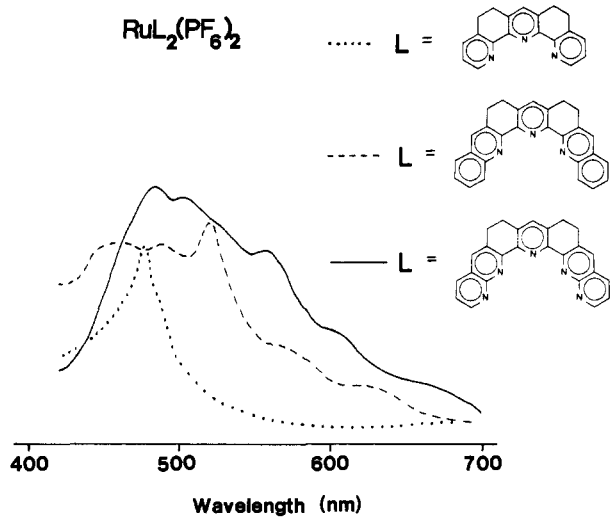

Figure 3. Electronic absorption spectra of ruthenium(II) complexes of bis(dimethylene)-bridged derivatives of 2,2′:6,2″-terpyridine.

mobile on the NMR time scale such that meso and *dl* forms were rapidly interconverting. As mentioned earlier, the tetramethylene-bridged species were conformationally rigid. Tridentate coordination results in the formation of two fused five-membered chelate rings and thus would be expected to diminish the ease of rotation about the 2,2′- and 6,2″-bonds. Furthermore, the meso form of the ligand, where the terminal aromatic rings are more nearly coplanar, would be expected to coordinate more readily.

For the RuL_2^{2+} complexes of **1b**, **2b**, and **3b** we observed two triplets for the dimethylene protons. The lower field triplet lies in the region 3.49–3.69 ppm and is assigned to the methylene group adjacent to the central pyridine ring, which should experience some small deshielding (more for **2b** and **3b**) from the terminal aromatic rings of the orthogonal ligand. The upper field triplet lies at 3.38–3.45 ppm and is assigned to the somewhat more shielded methylene protons adjacent to the terminal aromatic ring. Equivalency of the two protons at each position is explained by rapid inversion of the bridge on the NMR time scale, giving rise to the observed triplets by coupling with the adjacent methylene group.

For the ruthenium complexes of **1c**, **2c**, and **3c** the bridge protons show a triplet for each of the α-methylene groups and a quintet for the β-methylenes, again indicative of rapid inversion of the bridge. The relative chemical shifts of the two triplets may be explained in the same manner as for the dimethylene-bridged complexes. The quintet is upfield at 2.34–2.63 ppm. Interestingly, the α-methylene group adjacent to the terminal quinoline ring of **2c** appears at 2.26 ppm, a shift of about 1 ppm to higher field than the α-methylene of **1c** or **3c**. Examination of a molecular model shows this proton to be pointing toward the shielding face of the benzo portion of the orthogonal quinoline ring. Due to congestion caused by $H_{8'}$ and $H_{8''}$ of this ligand, the quinoline rings are probably skewed off the mean free plane of the ligand, pushing them toward these α-methylene protons. A similar effect is not observed for the naphthyridine analogue **3c**, where the absence of $H_8/H_{8''}$ protons relieves this congested situation.

For the tetramethylene-bridged systems, **1d**, **2d**, and **3d**, the complexity and overlap of the bridge proton signals even at 300 MHz does not allow any straightforward conclusion regarding the conformation of the bridges.

Although the additional constraints of complexation might have been expected to decrease conformational mobility of the bridges in the dimethylene and trimethylene bisannelated series, another important effect appears to be operative. The conformations of these ligands having all three aromatic rings coplanar ($\theta = 0°$, Table I) would in fact be the transition state for conformational inversion of the bridges. To the extent that these ligands "flatten out" as a result of coordination, the energy barrier to inversion will diminish and this process may, in fact, become more facile. Future studies will examine dynamic effects in these bridges as a function of temperature while computational techniques will be applied to an analysis of minimum-energy conformations.

Table III. Electronic Absorption Data for Ruthenium Complexes

complex	λ_{max},[a] nm (ϵ)		
$Ru(\mathbf{1a})_2^{2+}$	230 (38 400)	270 (42 800)	475 (16 200)
	240 (30 800)	280 (28 800)	
		310 (71 600)	
		330 (32 900)	
$Ru(\mathbf{1b})_2^{2+}$	235 (25 350)	295 (33 130)	415 (5810)
		310 (45 050)	475 (13 230)
		340 (27 580)	
		355 (38 080)	
$Ru(\mathbf{1c})_2^{2+}$	235 (48 280)	285 (34 980)	435 (6900)
		325 (60 890)	495 (14 290)
		345 (25 620)	
$Ru(\mathbf{1d})_2^{2+}$	230 (49 300)	285 (38 390)	495 (14 170)
		325 (60 500)	
$Ru(\mathbf{2a})_2^{2+}$	250 (74 680)	310 (44 380)	510 (8210)
		325 (37 810)	560 (4230)
		355 (29 850)	610 (1860)
		370 (44 780)	
$Ru(\mathbf{2b})_2^{2+}$	250 (91 630)	325 (49 360)	450 (6400)
		360 (24 140)	470 (6400)
		380 (37 800)	490 (6350)
		400 (60 690)	520 (7140)
			570 (2760)
			620 (1350)
$Ru(\mathbf{2c})_2^{2+}$	245 (67 820)	320 (45 150)	525 (9500)
	255 (70 500)	350 (40 100)	635 (2720)
		385 (22 970)	
$Ru(\mathbf{2d})_2^{2+}$	245 (45 740)	330 (33 170)	550 (6880)
	260 (50 300)	360 (29 900)	630 (2850)
$Ru(\mathbf{3a})_2^{2+}$	235 (60 780)	308 (47 550)	495 (7600)
	250 (53 920)	335 (32 840)	530 (8330)
		345 (35 290)	590 (5760)
		365 (35 010)	
$Ru(\mathbf{3b})_2^{2+}$	235 (46 130)	325 (46 500)	485 (8790)
		375 (31 960)	500 (8380)
		395 (56 960)	560 (6340)
$Ru(\mathbf{3c})_2^{2+}$	235 (45 050)	295 (25 520)	500 (6900)
	265 (28 130)	320 (42 970)	530 (7030)
		360 (34 010)	560 (6380)
		375 (28 910)	
$Ru(\mathbf{3d})_2^{2+}$	240 (52 980)	300 (28 800)	500 (7330)
	270 (31 410)	325 (44 500)	560 (8510)
		365 (39 010)	620 (5240)
		370 (37 430)	

[a] In CH_3CN.

Electronic Spectra. Table III summarizes the electronic absorption data for the RuL_2^{2+} complexes under discussion. The spectra consist of two well-defined regions. A relatively intense absorption generally consisting of two distinct bands is observed at shorter wavelength, 230–400 nm. This absorption is attributed to $\pi \rightarrow \pi^*$ transitions associated with the aromatic rings of the ligands themselves. A less intense, longer wavelength band in the region of 400–640 nm is assigned to the metal-to-ligand charge-transfer (MLCT) state. As the ligand is varied from **1** to **2** to **3**, its ability to delocalize charge becomes greater and the MLCT absorption envelope broadens in the direction of lower energy (see Figure 3). Somewhat surprisingly, we do not observe any dramatic or consistent variation in the position or intensities of the absorption maxima as a function of the length of the polymethylene bridge.

Two explanations are possible for this insensitivity to bridge length. Coordination may cause flattening of the ligands such that the dihedral angle between adjacent aromatic rings varies much less than in the free ligand. Alternatively, the MLCT state may be heavily centered on the two outermost rings (pyridine for **1**, quinoline for **2**, and 1,8-naphthyridine for **3**) such that delocalization into the central pyridine ring is of less importance and

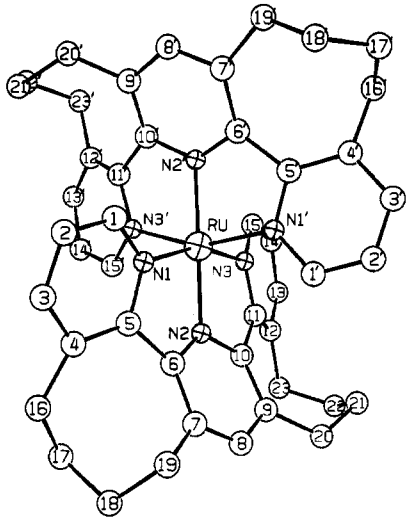

Figure 4. ORTEP drawing of $Ru(\mathbf{1d})_2[PF_6]_2$ with atomic numbering scheme.

hence noncoplanarity of this ring will not significantly affect the properties of the MLCT state.

X-ray Structure Determination

To help better understand the conformational demands of octahedral coordination on the geometry of our terpyridine ligands, we undertook a single-crystal X-ray analysis of the complex $Ru(\mathbf{1d})_2[PF_6]_2$. The pertinent geometric features of this complex are given in Table IV, while the atomic numbering scheme is included on the ORTEP plot in Figure 4.

The first important observation that can be made involves the shape of the coordinated ligand. In its uncomplexed form we estimate the dihedral angle between two adjacent pyridines to be about 80°. In its complexed form we observe the dihedral angle between the least-squares plane of two adjacent pyridines to vary from 31.1 to 35.8° with an average value of 33°. Thus there has been considerable flattening of the ligand but the system is still significantly nonplanar. Two interesting questions arise. Where and how is the "flattening" strain absorbed by the ligand and what are the conformations of the bridges?

The preponderance of the recent studies involving structural characterization of bis(2,2′:6,2″-terpyridyl)metal species have concentrated on complexes of cobalt(II).[17] Attention has also been focused on chromium(III)[18] and iron(II).[19] Although no structural determination has yet been reported for a bis(terpyridine)ruthenium(II) complex, two structures have recently been determined for mono(terpyridine)ruthenium(II) species.[20,21] White and co-workers have summarized some of the pertinent data on known bis(terpyridine) complexes, all of which exhibit a meridional disposition of the planar ligands around the metal center, resulting in substantial distortion of the octahedral geometry to accommodate the diminished N–M–N angles required by the two fused five-membered chelate rings.[22]

Examination of the ruthenium–nitrogen bond distances outlined in Table IV for $Ru(\mathbf{1d})_2[PF_6]_2$ shows these to average 1.996 Å for the central nitrogen and 2.050 Å for the distal nitrogens. These values are in good agreement with other structures involving nonannelated terpyridines.[22] The bond angles of the chelate rings also appear to be quite normal with an average N–Ru–N angle of 79.9°.[22]

Table IV. Pertinent Geometric Features of the $Ru(\mathbf{1d})_2[PF_6]_2$ Complex

Bond Lengths (Å)			
Ru–N1	2.062 (6)[a]	Ru–N1′	2.055 (6)
Ru–N2	1.994 (6)	Ru–N2′	1.997 (5)
Ru–N3	2.052 (6)	Ru–N3′	2.030 (6)
Bond Angles (deg)			
N1–Ru–N2	80.5	N1′–Ru–N2′	80.1
N2–Ru–N3	80.4	N2′–Ru–N3′	78.6

Torsion Angles (deg)	ligand A[b]	ligand B[b]
1. About the Inter-Pyridine Bond		
N1–C5–C6–N2	−23.9	−22.9
C4–C5–C6–C7	−36.4	−34.9
N2–C10–C11–N3	22.8	23.8
C5–C10–C11–C12	37.5	39.6
2. Interior to the Pyridine Rings		
N1–C1–C2–C3	−5.0	−3.4
C1–C2–C3–C4	2.7	4.8
C2–C3–C4–C5	5.6	2.2
C3–C4–C5–N1	−12.0	−10.6
C4–C5–N1–C1	10.4	12.4
C5–N1–C1–C2	−1.6	−5.4
ω[c]	37.3	38.8
N2–C6–C7–C8	−2.8	2.1
C6–C7–C8–C9	1.2	−2.4
C7–C8–C9–C10	−5.2	−5.3
C8–C9–C10–N2	10.7	12.7
C9–C10–N2–C6	−13.4	−14.0
C10–N2–C6–C7	9.2	6.2
ω	42.5	42.7
N3–C11–C12–C13	3.0	5.5
C11–C12–C13–C14	2.3	0.0
C12–C13–C14–C15	−5.8	−4.2
C13–C14–C15–N3	4.0	3.3
C14–C15–N3–C11	1.5	1.9
C15–N3–C11–C12	−4.9	−6.5
ω	21.5	21.4
3. About the Pyridine-Bridge Bond		
C5–C4–C16–C17 (distal)	0.6	96.0
C6–C7–C19–C18 (central)	87.7	−27.0
C10–C9–C20–C21 (central)	5.2	0.1
C11–C12–C23–C22 (distal)	−87.8	−88.4

[a] Numbers in parentheses are estimated standard deviations in the least significant figure. [b] A values are for the unprimed ligand, and B values are for the primed ligand. [c] ω = Σ|torsion angles| for each pyridine ring.

Although one might imagine that the meso form of **1d** could be capable of distorted facial complexation around ruthenium, the typical meridional disposition is, in fact, observed. The chelate rings are nevertheless highly perturbed in that the ruthenium atom is found to be considerably out of the planes of each of the pyridine rings. Planes 1–6 are designated as the least-squares best planes for the pyridine rings containing nitrogen atoms N1, N2, N3, N1′, N2′, and N3′, respectively. The ruthenium atom is found to be −0.457, 0.876, −0.498, −0.590, 0.814, and −0.584 Å out of these planes, respectively. These values are significantly greater than those found in the structure of bis(2,2′:6′,2″-terpyridine)iron(II) perchlorate hydrate,[19] where the deviations range from 0.047 to 0.134 Å. The highest degree of distortion is associated with the two central pyridine rings, planes 2 and 5.

We find, however, that while chelation tends to flatten the terpyridine geometry, the tetramethylene bridge counteracts this influence, resulting in considerable torsion about the 2,2′- and 6,2″-bonds connecting the pyridine rings. In the case of an unbridged terpyridine, one would expect the torsion angles about the C5–C6 bond defined as ∠N1–C5–C6–N2 and ∠C4–C5–C6–C7 to be identical and equal to zero for a planar system. These torsion angles for our complex are summarized in Table IV. The angles measured interior to the chelate ring measure an average of 23.4°

(17) Figgis, B. N.; Kucharski, E. S.; White, A. H. *Aust. J. Chem.* **1983**, *36*, 1527, 1537.
(18) Wickramasinghe, W. A.; Bird, P. H.; Jamieson, M. A.; Serpone, N. *J. Chem. Soc., Chem. Commun.* **1979**, 798.
(19) Baker, A. T.; Goodwin, H. A. *Aust. J. Chem.* **1985**, *38*, 207.
(20) Deacon, G. B.; Patrick, J. M.; Skelton, B. W.; Thomas, N. C.; White, A. H. *Aust. J. Chem.* **1984**, *37*, 929.
(21) Adcock, P. A.; Keene, F. R.; Smythe, R. S.; Snow, M. R. *Inorg. Chem.* **1984**, *23*, 2336.
(22) Figgis, B. N.; Kucharski, E. S.; White, A. H. *Aust. J. Chem.* **1983**, *36*, 1563.

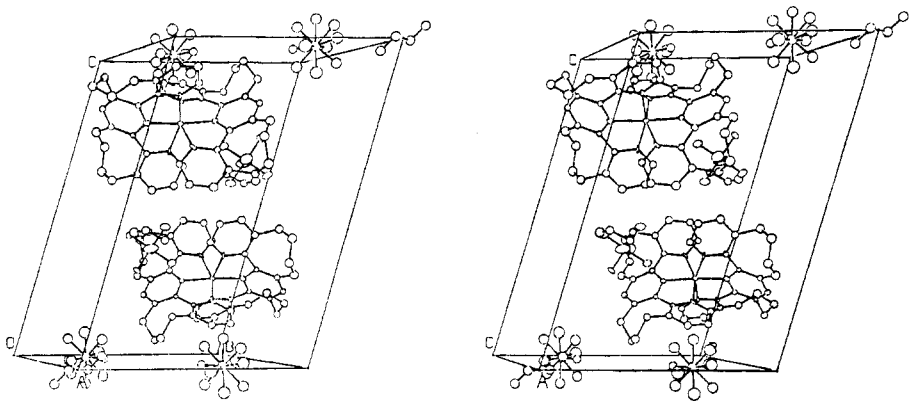

Figure 5. Stereoscopic representation of the Ru(**1d**)$[PF_6]_2$ unit cell (including a half-molecule of C_2H_5OH).

while those exterior to this ring average 37.1°. This difference of almost 14° can only be explained by considerable distortion from planarity of the pyridine rings themselves.

The relative planarity of the pyridine rings can be evaluated by comparison of their ω values, where ω equals the sum of the absolute values of the six interior torsion angles in the aromatic ring. For a completely planar ring $\omega = 0$. From the values of ω summarized in Table IV we see that all three rings are substantially distorted from planarity. There is very good agreement of the ω values when the two ligands denoted A (unprimed atoms) and B (primed atoms) are compared. The central pyridine ring, which participates in both chelate rings, is the most highly distorted. Surprisingly, the degrees of distortion in the two distal pyridine rings are significantly different. This observation implies that there might be differences in the conformations of the two tetramethylene bridges and the subsequent strain imposed by them on the attached pyridine rings.

This supposition is borne out when we examine the torsion angle data for the bond joining the pyridine ring to the α-carbon of the bridge (Table IV). The magnitude and sign of this angle will define the inherent chirality of the bridge. If we assume that the angle denoted as −27.0° for ligand B is in fact close to 0°, then the following picture develops. Ligand B shows approximate C_2 symmetry with the two bridges having mirror configurations while ligand A is dissymmetric so that one bridge lies above and one lies below the mean plane of the ligand. The terpyridine skeletons of both ligands adopt an approximate meso configuration. The anomalous shape of ligand A becomes readily apparent when one inspects the three-dimensional representation afforded by the stereoscopic drawing of the unit cell shown in Figure 5. At present we have no clear explanation for this unusual behavior.

Conclusions

From the above information we may draw the following conclusions. First, derivatives of 2,2′:6,2″-terpyridine and their dibenzo- and dipyrido-fused analogues will coordinate with ruthenium(II) in an octahedral fashion even when the conformation of the free ligand is highly distorted from planarity. NMR chemical shift data can be used as a sensitive probe of shielding and deshielding effects dependent upon the relative orientation of the terpyridine ligands about the metal atom. Coordination of ruthenium(II) with the bis(tetramethylene)-bridged terpyridine **1d** does not greatly alter the geometry of complexation at the metal center. Instead, the ligand distorts to accommodate coordination and a substantial degree of this distortion is manifested by nonplanarity in the individual pyridine rings. Despite these changes, which might be expected to affect the electronic properties of the complex, no dramatic differences are observed in the electronic absorptions as a function of bridge length.

We are continuing our investigations of the interrelationship between ligand conformation and coordination geometry.

Experimental Section

Nuclear magnetic resonance spectra were obtained on a Varian Associates FT-80 or a Nicolet NT-300 WB spectrometer and chemical shifts are reported in parts per million downfield from Me_4Si. Ultraviolet spectra were obtained on a Perkin-Elmer 330 spectrometer. Mass spectra were obtained by direct sample introduction into a Hewlett-Packard 5933A gas chromatograph–mass spectrometer while LC–MS measurements were performed on a Biospec mass spectrometer with a thermospray ionization interface. All solvents were freshly distilled reagent grade. The preparations of all ligands with the exception of **3a** have been described in an earlier paper.[3]

2,6-Di(2′-[1,8]naphthyridyl)pyridine (3a). To a mixture of 0.33 g (2 mmol) of 2,6-diacetylpyridine and 0.49 g (4 mmol) of 2-aminonicotinaldehyde[23] in 20 mL of absolute ethanol was added a solution of 0.05 g of KOH in 2 mL of absolute ethanol. The mixture was refluxed for 4 h under N_2 and cooled, and the precipitate was collected to provide 0.64 g (95%) of **3a**, mp >300 °C: ^{1}H NMR (80 MHz, $CDCl_3$) δ 9.27 (d, $H_{7'}$, J = 4.2 Hz), 9.11 (d, H_3, J = 7.2 Hz), 8.96–8.02 (m, $H_{3'}$, $H_{4'}$, $H_{5'}$, and H_4), 7.54 (dd, $H_{6'}$, J = 8.3, 4.0 Hz); IR (KBr) 3040, 1590, 1540, 1490, 1450, 1420, 1180, 890, 790 cm^{-1}; MS, *m/e* (relative intensity) 336 (15, M + 1), 335 (61, M), 207 (37), 206 (100), 179 (30), 129 (19).

General Procedure for the Preparation of Ruthenium Complexes. A solution of the ligand (2.5 equiv) and ruthenium trichloride trihydrate (1.0 equiv) in ethanol–water (1:1) was refluxed for 6–48 h until the solution became red or purple, indicating formation of RuL_2Cl_2. After cooling, the insoluble materials were removed by filtration and the complex was precipitated by the addition of aqueous ammonium hexafluorophosphate (2 equiv). The complexes were purified either by direct recrystallization from acetonitrile–toluene (1:1) (method A) or by chromatography on neutral alumina with acetonitrile–toluene (1:1) as eluent, followed by crystallization from this eluting solvent mixture (method B).

Ru(1b)$_2$[PF$_6$]$_2$. Treatment of 0.29 g of **1b** with $RuCl_3$ for 6 h provided 0.35 g (91%) of the complex purified by method A: ^{1}H NMR (300 MHz, CD_3CN) δ 7.83 (s, H_4), 7.62 (dd, $H_{4'}$, $J_{4',5'}$ = 7.7 Hz, $J_{4',6'}$ = 1.0 Hz), 7.17 (dd, $H_{6'}$, $J_{5',6'}$ = 5.9 Hz), 7.03 (dd, $H_{5'}$), 3.49 (t, α-CH_2, J = 7.3 Hz), 3.38 (t, α-CH_2, J = 7.3 Hz); LC–MS, *m/e* (relative intensity) 667 (RuL_2^+ − 4, 49), 331 (RuL_2^{2+} − 4, 9), 281 (L − 4, 100).

Ru(1c)$_2$[PF$_6$]$_2$. Treatment of 0.21 g of **1c** with $RuCl_3$ for 12 h provided 0.23 g (66%) of the complex purified by method A: ^{1}H NMR (300 MHz, CD_3CN) δ 7.94 (s, H_4), 7.63 (d, $H_{4'}$, $J_{4',5'}$ = 8.0 Hz), 7.13 (d, $H_{6'}$, $J_{5',6'}$ = 5.5 Hz), 7.00 (dd, $H_{5'}$), 3.40 (t, α-CH_2, J = 6.7 Hz), 3.19 (t, α-CH_2, J = 6.3 Hz), 2.34 (quintet, β-CH_2); ^{13}C NMR (20 MHz, CD_3CN) 158.3/153.4 (C_2, $C_{2'}$), 150.2 ($C_{6'}$), 143.0/142.2 (C_3, $C_{3'}$), 141.5 (C_4), 141.1 ($C_{4'}$), 126.9 ($C_{5'}$), 36.1/35.8 (α-C), 26.2 (β-C).

Ru(1d)$_2$[PF$_6$]$_2$. Treatment of 0.25 g of **1d** with $RuCl_3$ for 12 h provided 0.29 g (85%) of the complex purified by method A: ^{1}H NMR (300 MHz, CD_3CN) δ 7.84 (s, 4 H), 7.64 (dd, $H_{4'}$, $J_{4',5'}$ = 8.1 Hz, $J_{4',6'}$ = 1.7 Hz), 7.05 (dd, $H_{5'}$, $J_{5',6'}$ = 5.1 Hz), 6.90 (broad s, H_6), 3.25 (d, 4 H), 3.09 (m, 2 H), 2.26 (broad s, 2 H), 1.93 (m, 2 H); ^{13}C NMR (20 MHz, CD_3CN) 158.4/154.4 (C_2, $C_{2'}$), 150.5 ($C_{6'}$), 143.2 (C_4), 142.4/141.7 (C_3, $C_{3'}$), 141.2 ($C_{4'}$), 127.0 ($C_{5'}$), 33.4/34.0 (α-C), 26.0/24.6 (β-C).

Ru(2a)$_2$[PF$_6$]$_2$. Treatment of 0.15 g of **2a** with $RuCl_3$ for 24 h provided 0.09 g (55%) of the complex purified by method A: ^{1}H NMR (300 MHz, CD_3CN) δ 9.14 (d, H_3, H_5, $J_{3,4}$ = 8.2 Hz), 8.84 (t, H_4), 8.38 (d, $H_{3'}$ or $H_{4'}$, $J_{3',4'}$ = 8.6 Hz), 8.28 (d, $H_{3'}$ or $H_{4'}$), 7.77 (dd, $H_{5'}$, $J_{5',6'}$ = 8.2 Hz, $J_{5',7'}$ = 2.1 Hz), 7.53 (t, $H_{6'}$ or $H_{7'}$, $J_{6',7'}$ = 7.0 Hz), 7.27 (t, $H_{6'}$ or $H_{7'}$), 6.52 (d, $H_{8'}$, $J_{7',8'}$ = 9.0 Hz).

Ru(2b)$_2$[PF$_6$]$_2$. Treatment of 0.21 g of **2b** with $RuCl_3$ for 24 h provided 0.025 g (15%) of the complex purified by method B, but with chromatography on silica gel: ^{1}H NMR (300 MHz, CD_3CN) δ 8.40 (s, H_4), 8.02 (s, $H_{4'}$), 7.66 (dd, $H_{5'}$, $J_{5',6'}$ = 8.0 Hz, $J_{5',7'}$ = 2.0 Hz), 7.44 (t,

(23) Majewicz, T. G.; Caluwe, P. *J. Org. Chem.* **1974**, *39*, 720.

Table V. X-ray Data Collection and Processing Parameters for $Ru(\mathbf{1d})_2[PF_6]_2$

molecular formula	$RuP_2F_{12}ON_6C_{48}H_{52}$
fw	1120.0
space group	$P\bar{1}$, triclinic
cell constants	a = 10.237 (1) Å
	b = 13.250 (1) Å
	c = 19.761 (3) Å
	α = 73.59 (1)°
	β = 89.59 (1)°
	γ = 72.22 (1)°
	V = 2439 Å^3
formula units/cell	Z = 2
density	ρ = 1.53 g/cm^3
abs coeff	μ = 4.65 cm^{-1}
radiation (Mo Kα)	λ = 0.71073 Å
collecn range	$4° \le 2\theta \le 30°$
scan width	$\Delta\theta = (1.00 + 0.35 \tan\theta)°$
max scan time	120 s
scan speed range	0.7–5.0°/min
total data collected	1894
independent data, $I > 3\sigma(I)$	1578
total variables	380
$R = \sum\|\|F_o\| - \|F_c\|\|/\sum\|F_o\|$	0.065
$R_w = [\sum w(\|F_o\| - \|F_c\|)^2/\sum w\|F_o\|^2]^{1/2}$	0.075
wts	$w = \sigma(F)^{-2}$

$H_{6'}$ or $H_{7'}$, $J_{6',7'}$ = 6.8 Hz), 7.33 (t, $H_{6'}$ or $H_{7'}$), 6.58 (d, $H_{8'}$, $J_{7',8'}$ = 9.0 Hz), 3.69 (t, α-CH_2, J = 7.5 Hz), 3.38 (t, α-CH_2); LC–MS, m/e (relative intensity 868 (RuL_2^+ – 4, 15), 385 (L, 100).

$Ru(\mathbf{2c})_2[PF_6]_2$. Treatment of 0.20 g of **2c** with $RuCl_3$ for 48 h provided 0.06 g (26%) of the complex purified by method B: ^{1}H NMR (300 MHz, CD_3CN) δ 8.30 (s, H_4), 7.77 (s, $H_{4'}$), 7.71 (dd, $H_{5'}$, $J_{5',6'}$ = 8.2 Hz, $J_{5',7'}$ = 1.9 Hz), 7.50 (t, $H_{6'}$ or $H_{7'}$, $J_{6',7'}$ = 7.5 Hz), 7.21 (t, $H_{6'}$ or $H_{7'}$), 6.42 (d, $H_{8'}$, $J_{7',8'}$ = 7.8 Hz), 3.32 (t, α-CH_2, J = 7 Hz), 2.38 (m, β-CH_2), 2.26 (t, α-CH_2).

$Ru(\mathbf{2d})_2[PF_6]_2$. Treatment of 0.10 g of **2d** with $RuCl_3$ for 48 h provided 0.04 g (35%) of the complex purified by method B: ^{1}H NMR (80 MHz, CD_3CN) δ 8.24 (s, H_4), 7.73 (s, $H_{4'}$), 7.66–7.09 (overlapping m, $H_{5'}$, $H_{6'}$, and $H_{7'}$), 6.42 (d, $H_{8'}$, $J_{7',8'}$ = 8.6 Hz), 3.2–2.0 (broad overlapping m, $-CH_2-$).

$Ru(\mathbf{3a})_2[PF_6]_2$. Treatment of 0.30 g of **3a** with $RuCl_3$ for 48 h provided 0.17 g (35%) of the complex purified by method A: ^{1}H NMR (300 MHz, CD_3CN) δ 9.08 (d, H_3, $J_{3,4}$ = 8.1 Hz), 8.66 (t, H_4), 8.53 (d, $H_{3'}$, $J_{3',4}$ = 8.6 Hz), 8.28 (d, $H_{4'}$), 8.18 (d, $H_{7'}$, $J_{6',7'}$ = 4.2 Hz), 8.09 (dd, $H_{5'}$, $J_{5',6'}$ = 8.2 Hz, $J_{5',7'}$ = 2.7 Hz), 7.35 (dd, $H_{6'}$).

$Ru(\mathbf{3b})_2[PF_6]_2$. Treatment of 0.40 g of **3b** with $RuCl_3$ for 36 h provided 0.35 g (75%) of the complex purified by method A: ^{1}H NMR (300 MHz, CD_3CN) δ 8.23 (dd, $H_{7'}$, $J_{6',7'}$ = 4.2 Hz, $J_{5',7'}$ = 2.0 Hz), 8.15 (s, H_4), 7.99 (dd, $H_{5'}$, $J_{5',6'}$ = 8.1 Hz), 7.97 (s, $H_{4'}$), 7.29 (dd, $H_{6'}$), 3.65 (t, α-CH_2, J = 7.8 Hz), 3.45 (t, α-CH_2); LC–MS, m/e (relative intensity) 873 (RuL_2^+ – 2, 15), 434 (RuL_2^{2+} – 3, 41).

$Ru(\mathbf{3c})_2[PF_6]_2$. Treatment of 0.28 g of **3c** with $RuCl_3$ for 48 h provided 0.25 g (89%) of the complex purified by method A: ^{1}H NMR (300 MHz, CD_3CN) δ 8.28 (s, H_4), 8.26 (dd, $H_{7'}$, $J_{6',7'}$ = 4.3 Hz, $J_{5',7'}$ = 1.8 Hz), 8.04 (dd, $H_{5'}$, $J_{5',6'}$ = 8.1 Hz), 8.01 (s, $H_{4'}$), 7.34 (dd, $H_{6'}$), 3.30 (t, α-CH_2, J = 7.1 Hz), 3.01 (t, α-CH_2, J = 6.7 Hz), 2.63 (quintet, β-CH_2); LC–MS, m/e (relative intensity) 927 (RuL_2^+ – 4, 37), 465 (RuL_2^{2+}, 85), 419 (52), 315 (81), 236 (64).

$Ru(\mathbf{3d})_2[PF_6]_2$. Treatment of 0.20 g of **3d** with $RuCl_3$ for 48 h provided 0.05 g (20%) of the complex purified by method B: ^{1}H NMR (300 MHz, CD_3CN) δ 8.27 (dd, $H_{7'}$, $J_{6',7'}$ = 4.2 Hz, $J_{5',7'}$ = 1.8 Hz), 8.16 (s, H_4), 7.96 (dd, $H_{5'}$, $J_{5',6'}$ = 8.1 Hz), 7.91 (s, $H_{4'}$), 7.30 (dd, $H_{6'}$), 3.23 (m, 4 H), 2.88 (m, 4 H), 2.00 (m, 8 H); LC–MS, m/e (relative intensity) 985 (RuL_2^+ – 2, 11), 493 (RuL_2^{2+}, 100), 418 (74), 279 (76).

X-ray Determination. A large reddish purple tabular block of $Ru(\mathbf{1d})_2[PF_6]_2$ crystallized from acetonitrile–ethanol, 0.50 × 0.30 × 0.30 mm, was mounted on a glass fiber in a random orientation on an Enraf-Nonius CAD-4 automatic diffractometer. The radiation used was Mo Kα monochromatized by a dense graphite crystal assumed for all

Table VI. Positional Parameters and Their Estimated Standard Deviations (in Parentheses)[a]

atom	x	y	z	atom	x	y	z
Ru	0.0509 (2)	0.8481 (1)	0.26009 (9)	C12	0.311 (2)	0.886 (2)	0.405 (1)
P1	0.7471 (7)	0.7313 (5)	0.9952 (4)	C13	0.364 (2)	0.782 (2)	0.454 (1)
P2	0.3690 (8)	0.3882 (5)	0.3608 (3)	C14	0.345 (2)	0.693 (2)	0.442 (1)
F1	0.865 (2)	0.635 (1)	0.9854 (9)	C15	0.262 (2)	0.706 (2)	0.383 (1)
F2	0.628 (1)	0.836 (1)	1.0004 (7)	C16	−0.367 (2)	1.238 (2)	0.161 (1)
F3	0.723 (3)	0.781 (2)	0.911 (2)	C17	−0.307 (2)	1.292 (2)	0.202 (1)
F4	0.624 (2)	0.684 (2)	0.993 (1)	C18	−0.215 (2)	1.356 (2)	0.167 (1)
F5	0.870 (3)	0.768 (2)	1.006 (2)	C19	−0.103 (2)	1.284 (2)	0.133 (1)
F6	0.751 (3)	0.695 (2)	1.080 (1)	C20	0.343 (2)	1.116 (2)	0.275 (1)
F3′	0.790 (3)	0.829 (2)	0.935 (1)	C21	0.468 (2)	1.021 (2)	0.314 (1)
F4′	0.667 (3)	0.709 (2)	0.934 (1)	C22	0.466 (2)	1.002 (2)	0.392 (1)
F5′	0.836 (3)	0.752 (2)	1.051 (1)	C23	0.342 (2)	0.983 (2)	0.423 (1)
F6′	0.725 (3)	0.631 (2)	1.054 (1)	C1′	0.252 (2)	0.901 (2)	0.155 (1)
F7	0.350 (2)	0.359 (1)	0.2911 (7)	C2′	0.365 (2)	0.871 (2)	0.117 (1)
F8	0.354 (2)	0.277 (1)	0.4067 (7)	C3′	0.413 (2)	0.766 (2)	0.114 (1)
F9	0.215 (1)	0.450 (1)	0.3614 (8)	C4′	0.343 (2)	0.689 (1)	0.143 (1)
F10	0.385 (2)	0.502 (1)	0.3152 (6)	C5′	0.220 (2)	0.727 (1)	0.1735 (9)
F11	0.527 (2)	0.332 (1)	0.3616 (8)	C6′	0.120 (2)	0.667 (1)	0.2011 (9)
F12	0.396 (1)	0.416 (1)	0.4312 (6)	C7′	0.080 (2)	0.588 (1)	0.175 (1)
O1	0.148 (5)	0.871 (3)	0.587 (2)	C8′	−0.029 (2)	0.560 (1)	0.203 (1)
O2	0.003 (5)	0.915 (3)	−0.042 (2)	C9′	−0.102 (2)	0.598 (2)	0.256 (1)
N1	−0.115 (2)	0.943 (1)	0.1872 (8)	C10′	−0.052 (2)	0.662 (1)	0.286 (1)
N2	0.048 (1)	1.000 (1)	0.2590 (7)	C11′	−0.095 (2)	0.709 (1)	0.344 (1)
N3	0.208 (1)	0.807 (1)	0.3368 (8)	C12′	−0.138 (2)	0.651 (2)	0.406 (1)
N1′	0.186 (2)	0.829 (1)	0.1839 (7)	C13′	−0.170 (2)	0.705 (2)	0.458 (1)
N2′	0.048 (2)	0.702 (1)	0.2522 (7)	C14′	−0.158 (2)	0.807 (2)	0.450 (1)
N3′	−0.073 (1)	0.807 (1)	0.3369 (7)	C15′	−0.105 (2)	0.856 (1)	0.388 (1)
C1	−0.189 (2)	0.904 (1)	0.154 (1)	C16′	0.401 (2)	0.571 (2)	0.139 (1)
C2	−0.313 (2)	0.973 (2)	0.115 (1)	C17′	0.360 (2)	0.560 (2)	0.068 (1)
C3	−0.361 (2)	1.081 (2)	0.118 (1)	C18′	0.211 (2)	0.590 (2)	0.058 (1)
C4	−0.287 (2)	1.123 (1)	0.155 (1)	C19′	0.140 (2)	0.532 (2)	0.117 (1)
C5	−0.155 (2)	1.054 (1)	0.1843 (9)	C20′	−0.238 (2)	0.577 (2)	0.268 (1)
C6	−0.045 (2)	1.089 (1)	0.2125 (9)	C21′	−0.344 (2)	0.626 (2)	0.316 (1)
C7	−0.011 (2)	1.188 (1)	0.1882 (9)	C22′	−0.299 (2)	0.557 (2)	0.391 (1)
C8	0.108 (2)	1.189 (1)	0.215 (1)	C23′	−0.156 (2)	0.542 (2)	0.418 (1)
C9	0.203 (2)	1.100 (1)	0.264 (1)	C24	0.050 (3)	0.941 (2)	0.002 (2)
C10	0.164 (2)	1.004 (1)	0.291 (1)	C25	0.080 (4)	0.755 (3)	0.613 (2)
C11	0.234 (2)	0.898 (1)	0.344 (1)	C26	0.064 (4)	0.859 (3)	0.583 (2)

[a] Hydrogen atom positions are given in the supplementary material.

purposes to be 50% imperfect. The Laue symmetry was determined to be 1, and from the systematic absences noted the space group was shown to be either $P1$ or $P\bar{1}$. Intensities were measured by using the θ-2θ scan technique, with the scan rate depending on the net count obtained in rapid prescans of each reflection. Data in the hemisphere of reciprocal space having $h \geq 0$ were collected. Two standard reflections were monitored periodically during the course of the data collection as a check of crystal stability and electronic reliability, and these showed some slight decay near the end of the experiment. Since this decay was not linear with time, no attempt was made to correct for it. In reduction of the data, Lorentz and polarization factors were applied; however, no correction for absorption was made due to the small absorption coefficient. No extinction correction was made.

The structure was solved by the Patterson method, which revealed the positions of the Ru atom. The remaining non-hydrogen atoms were found in subsequent difference Fourier syntheses. There are two PF_6^- anions in the asymmetric unit, one of which is ordered while the other exhibits a 50:50 disorder of four of the F positions about a central P site. Additionally, there is 1 equiv of ethanol present as solvent of crystallization, which occurs as one molecule having a 50% population factor in a general position and a second molecule having full-weight carbons and half-weight oxygens situated on an inversion center bisecting the carbon–carbon bond. The observed decay was most likely due to the gradual loss of ethanol from the lattice sites. The usual sequence of isotropic and anisotropic refinement was followed, after which all hydrogens were entered in ideally calculated positions. Hydrogen isotropic temperature factors were estimated on the basis of the thermal motion of the associated carbons. After all shift/esd ratios were less than 0.3, convergence was reached. No unusually high correlations were noted between any of the variables in the last cycle of least-squares refinement, and the final difference density map showed a maximum peak of about 1 e/Å^3, located near the ordered ethanol. Since no attempt was made to position hydrogens on these solvent molecules, this excess density is probably attributable to those missing atoms. The atomic scattering factors for the non-hydrogen atoms were computed from numerical Hartree–Fock wave functions;[24] for hydrogen those of Stewart, Davidson, and Simpson[25] were used. The anomalous dispersion coefficients of Cromer and Liberman[26] were used for Ru. All calculations were made with use of Molecular Structure Corp.'s TEXRAY 230 modifications of the SDP-PLUS series of programs. The data collection and processing parameters are outlined in Table V, and the positional parameters and their standard deviations are included in Table VI.

Acknowledgment. Financial support from the Robert A. Welch Foundation and the Petroleum Research Fund, administered by the American Chemical Society, is gratefully acknowledged. We also wish to thank the University of Houston NMR Institute for help in obtaining the 300-MHz NMR spectra and Dr. James Korp for assistance in the X-ray crystal analysis.

Registry No. Ru(**1b**)$_2$[PF$_6$]$_2$, 102588-55-6; Ru(**1c**)$_2$[PF$_6$]$_2$, 102575-96-2; Ru(**1d**)$_2$[PF$_6$]$_2$, 102575-99-5; Ru(**2a**)$_2$[PF$_6$]$_2$, 102576-00-1; Ru(**2b**)$_2$[PF$_6$]$_2$, 102576-02-3; Ru(**2c**)$_2$[PF$_6$]$_2$, 102588-57-8; Ru(**2d**)$_2$[PF$_6$]$_2$, 102576-04-5; **3a**, 102576-05-6; Ru(**3a**)$_2$[PF$_6$]$_2$, 102576-07-8; Ru(**3b**)$_2$[PF$_6$]$_2$, 102576-09-0; Ru(**3c**)$_2$[PF$_6$]$_2$, 102576-11-4; Ru(**3d**)$_2$[PF$_6$]$_2$, 102588-59-0; 2,6-diacetylpyridine, 1129-30-2; 2-aminonicotinaldehyde, 7521-41-7.

Supplementary Material Available: Tables pertinent to the X-ray crystallographic determination of Ru(**1d**)$_2$[PF$_6$]$_2$ including hydrogen atom positions, bond lengths, bond angles, least-squares planes, and refined and general temperature factor expressions (10 pages). Ordering information is given on any current masthead page.

(24) Cromer, D. T.; Mann, J. B. *Acta Crystallogr., Sect. A: Cryst. Phys., Diffr., Theor. Gen. Crystallogr.* **1968**, *A24*, 321.
(25) Stewart, R. F.; Davidson, E. R.; Simpson, W. T. *J. Chem. Phys.* **1965**, *42*, 3175.
(26) Cromer, D. T.; Liberman, D. *J. Chem. Phys.* **1970**, *53*, 1891.

Contribution from the Department of Chemistry, University of South Carolina, Columbia, South Carolina 29208

Facile Addition of Small Molecules to $Os_4(CO)_{12}(\mu_3\text{-}S)$. Syntheses and Crystal and Molecular Structures of $Os_4(CO)_{12}(NHMe_2)(\mu_3\text{-}S)$ and $Os_4(CO)_{12}(\mu\text{-}H)_2(\mu_3\text{-}S)$

Richard D. Adams* and Suning Wang

Received December 3, 1985

The cluster compound $Os_4(CO)_{12}(\mu_3\text{-}S)$ (**1**) undergoes facile addition reactions with the Lewis donors Me_2NH and CO to form the 1:1 adducts $Os_4(CO)_{12}(NHMe_2)(\mu_3\text{-}S)$ (**3**) and $Os_4(CO)_{13}(\mu_3\text{-}S)$ (**4**) in 96 and 54% yields, respectively. **1** undergoes addition of hydrogen at 105 °C to yield the dihydride $Os_4(CO)_{12}(\mu\text{-}H)_2(\mu_3\text{-}S)$ (**5**) in 56% yield. The molecular structures of **3** and **5** were determined by single-crystal X-ray diffraction analyses. For **3**, space group $P2_1/n$, a = 8.782 (1) Å, b = 25.162 (6) Å, c = 10.790 (2) Å, β = 109.39 (1)°, Z = 4, and ρ_{calcd} = 3.43 g/cm^3. The structure was solved by direct methods and refined (2328 reflections, $F^2 \geq 3.0\sigma(F^2)$) to the final values for the residuals R_F = 0.029 and R_{wF} = 0.033. The structure of **3** consists of a nearly planar butterfly tetrahedral cluster of four osmium atoms with a sulfido ligand bridging a closed triangle of three osmium atoms and a $NHMe_2$ ligand coordinated to the fourth osmium atom. For **5**, space group $P2_1/m$, a = 7.320 (1) Å, b = 17.097 (3) Å, c = 8.155 (1) Å, β = 104.79 (2)°, Z = 2, and ρ_{calcd} = 3.80 g/cm^3. The structure of **5** was solved by a combination of Patterson and difference Fourier techniques and was refined (1283 reflections, $F^2 \geq 3.0\sigma(F^2)$) to the final values of the residuals R_F = 0.051 and R_{wF} = 0.060. The structure of **5** consists of a butterfly tetrahedral cluster of four osmium atoms with a sulfido ligand bridging one of the open triangular faces. The molecule contains a crystallographically imposed plane of symmetry. Investigations of the compound $Os_4(CO)_{12}(\mu_3\text{-}NMe)$ (**2**), which is structurally analogous to **1**, revealed a surprising lack of reactivity for the additions corresponding to **1**. Possible mechanisms for the additions to **1** and the differences in reactivity between **1** and **2** are discussed.

Introduction

The ability to add and "activate" selected small molecules is a property that is essential for the development of transition-metal cluster compounds as catalysts.[1-4] Additions to coordinatively unsaturated compounds are usually very facile simply because ligand displacements are not required, but in the area of cluster chemistry stable unsaturated complexes are an unusual occurrence.[1,2,5] Unsaturation in cluster complexes is usually eliminated through the formation of metal–metal bonds. If, however, a metal–metal bond can be opened, unsaturation can be generated and ligand addition may then occur (e.g. eq 1).[6]

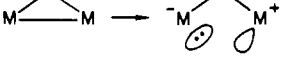

(1)

Although the unsymmetric cleavage of a homopolar metal–metal bond will result in a charge separation (eq 1), the cleavage

(1) Adams, R. D.; Horvath, I. T. *Prog. Inorg. Chem.* **1985**, *33*, 127.
(2) Kaesz, H. D. In *Metal Clusters in Catalysis*; Knozinger, H., Gates, B. C., Guczi, L., Eds.; Elsevier: Amsterdam, in press.
(3) Muetterties, E. L. *Catal. Rev.—Sci. Eng.* **1981**, *23*, 69.
(4) Muetterties, E. L.; Burch, R. R.; Stolzenberg, A. M. *Annu. Rev. Phys. Chem.* **1982**, *33*, 89.
(5) *Transition Metal Clusters*; Johnson, B. F. G., Ed., Wiley: Chichester, England, 1980.
(6) (a) Meyer, T. J. *Prog. Inorg. Chem.* **1975**, *19*, 1. (b) Vahrenkamp, H. *Philos. Trans. R. Soc. London, A* **1982**, *308*, 17. (c) Johnson, B. F. G.; Lewis, J. *Philos. Trans. R. Soc. London, A* **1982**, *308*, 5.

0020-1669/86/1325-2534$01.50/0